Electronic structure and magnetic properties of (Mn, N)-codoped ZnO*

Wang Qian-Jin(王前进)[a], Wang Jin-Bin(王金斌)[b]†, Zhong Xiang-Li(钟向丽)[b], Tan Qiu-Hong(谭秋红)[a], and Liu Ying-Kai(刘应开)[a]

[a] College of Physics and Electronic Information, Yunnan Normal University, Kunming 650500, China
[b] Faculty of Materials, Optoelectronics and Physics, Xiangtan University, Xiangtan 411105, China

(Received 17 April 2014; revised manuscript received 10 July 2014; published online 10 October 2014)

The electronic structures and magnetic properties of (Mn, N)-codoped ZnO are investigated by using the first-principles calculations. In the ferromagnetic state, as N substitutes for the intermediate O atom of the nearest neighboring Mn ions, about 0.5 electron per Mn^{2+} ion transfers to the N^{2-} ion, which leads to the high-state Mn ions (close to +2.5) and trivalent N^{3-} ions. In an antiferromagnetic state, one electron transfers to the N^{2-} ion from the downspin Mn^{2+} ion, while no electron transfer occurs for the upspin Mn^{2+} ion. The (Mn, N)-codoped ZnO system shows ferromagnetism, which is attributed to the hybridization between Mn 3d and N 2p orbitals.

Keywords: first-principles calculations, ferromagnetism, hybridization

PACS: 31.15.E, 71.55.Gs, 75.30.Hx **DOI:** 10.1088/1674-1056/23/12/123101

1. Introduction

ZnO-based diluted magnetic semiconductors (DMSs) have been attracting much attention for their potential applications in spintronic devices, but low Curie temperature (T_C) restricts their extensive applications. In 2000, Dietl *et al.*[1] predicted that T_C could be raised above room temperature in Mn-doped p-type ZnO with high carrier concentration. Motivated by the prediction, many efforts have been made to investigate the (Mn, N)-codoped ZnO system, for nitrogen is considered to be a good candidate for p-type dopant. Even though room-temperature ferromagnetisms in (Mn, N)-codoped ZnO films prepared by various techniques have been investigated,[2–10] the magnetic interaction mechanism is still unclear. Moreover, most theoretical research[11–13] adopts the local density approximation (LDA) or generalized gradient approximation (GGA), which fails to describe strongly correlated electron systems due to large inter-atomic self-interaction errors. The LDA/GGA + U method takes into account the orbital dependence of the Coulomb and can improve the description of the d states in a magnetic semiconductor. Therefore, in order to test the reliability of the results, the two schemes are necessary. In addition, when Mn and N ions are incorporated into ZnO lattice, how do the chemical states of Mn and N change? And how do they affect the magnetic state? About these questions, there has been no clear physical picture to date and so a theoretical investigation is highly desirable.

In this paper, we will investigate the electronic structures, magnetic properties, and the chemical states of doped ions in (Mn, N)-codoped ZnO systems with both GGA and GGA + U schemes, and also elaborate on the exchange interaction between magnetic ions.

2. Computation details

The calculations are carried out with the plane-wave basis set and ultrasoft pseudopotentials as implemented in the QUANTUM-ESSPRESO package,[14] and the generalized gradient approximation (GGA) functional in the form of Perdew–Burke–Ernzherof[15] (PBE) is employed. The wave functions are expanded by plane waves up to a cutoff energy of 60 Ry (1 Ry = 13.6056923 eV). Brillouin zone integration is performed by 4×4×4 Monkhorst and Pack special point grids[16,17] and Methfessel and Paxton smearing technique with a smearing width of 0.005 Ry.[18] All atoms are allowed to relax until the atomic force is smaller than 10^{-3} Ry/bohr. The ZnO supercell we investigated consists of 48 atoms. Two Zn ions are chosen to be substituted with two Mn ions in the supercell, which is equivalent to an Mn concentration of 8.3% ($Zn_{0.917}Mn_{0.083}O$). We study five different doping configurations of Mn-doped ZnO (see Fig. 1 and Table 1). Total energy calculations demonstrate that the two Mn ions tend to substitute for the nearest neighboring Zn ions, so we mainly investigate two configurations of Mn–N–Mn complex. One configuration is that the two Mn ions substitute for Zn ions at sites 1 and 3 (Mn–N–Mn chain along c axis), named C-1; and the other is that the two Mn ions substitute for Zn ions at sites 1 and 2, named C-2, as shown in Fig. 2(a). In the GGA + U

*Project supported by the National Natural Science Foundation of China (Grant Nos. 11304273, 10764005, 11164034, 11072208, and 11032010), the Yunnan Provincial Natural Science Foundation, China (Grant No. 2010DC053), and the Scientific Research Foundation for Ph. D. Student of Yunnan Normal University.

†Corresponding author. E-mail: jbwang@xtu.edu.cn

© 2014 Chinese Physical Society and IOP Publishing Ltd

scheme, we select $U_{Zn} = 2$ eV which is fitted by Hu *et al.*[19] and $U_{Mn} = 3$ eV.

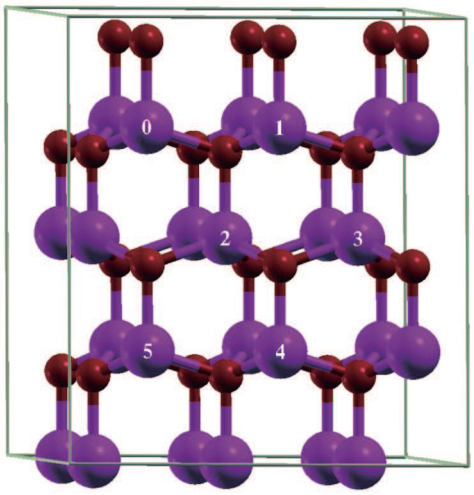


Fig. 1. (color online) Crystal structure of ZnO. The big (pink) and small (gray) balls represent the Zn and O atoms. The number marked on the atom refers to the number of other atoms that will substitute for the number-marked atom.

Table 1. Calculated results of different doping configurations in Mn-doped ZnO. The first column shows the different doping configurations, the second column the ground state of each doping configuration, the last column the energy difference between the ground state of each configuration and the ground state of the system, i.e., AFM state of configuration (0, 1).

Configuration (i, j)	Ground state	Relative energy ΔE/meV
(0, 1)	AFM	0
(0, 2)	AFM	17.68
(0, 3)	AFM	76.16
(0, 4)	AFM	77.52
(0, 5)	AFM	72.08

3. Results and discussion

Firstly, we investigate the properties of N-doped ZnO because some groups[20–22] reported in recent years that N-doped ZnO can induce magnetism. We consider a single anion O substituted by one N atom (N_O) in the 48-ion supercell. Results show that each N dopant introduces a total magnetic moment of 0.78 μ_B/supercell (~ 0.44 μ_B from N itself, ~ 0.34 μ_B from its 10 second-nearest-neighboring O atoms and its nearest-neighboring Zn atoms). Shen *et al.*[20] pointed out that the magnetism is the strong interaction between N 2p and the second-nearest-neighboring O 2p states at the Fermi level. Figure 2(b) shows the corresponding spatial spin distribution of N-doped ZnO in spin-polarized state. We expect that the spin-polarized N atom may play an important role in mediating the exchange interaction between the two Mn ions in (Mn, N)-codoped ZnO.

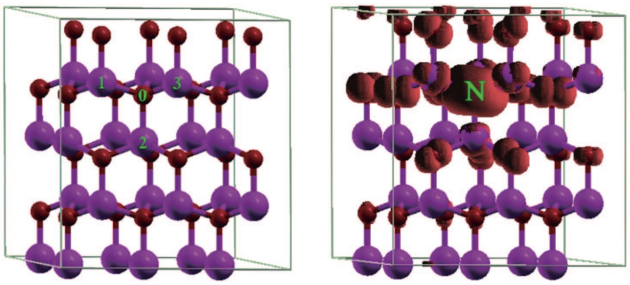


Fig. 2. (color online) (a) Side view of the schematic ZnO supercell consisting of 24 O atoms (small) and 24 Zn atoms (big). The number marked on the atom refers to the number of other atoms that will substitute for the number-marked atom. (b) The spatial spin distribution of N-doped ZnO in the 48-ion supercell, ($\rho = 8 \times 10^{-4}$ e/au^3), the unit au is the abbreviation for atomic unit.

Secondly, we study the C-1 and C-2 configurations in (Mn, N)-codoped ZnO. In the two configurations, both the ferromagnetic (FM) and antiferromagnetic (AFM) orderings are calculated, and the energy difference ΔE_{AFM-FM} between the AFM and FM spin orderings indicates that the lower one is for the ground magnetic ordering. Table 2 shows the magnetic moments and the values of energy difference ΔE_{AFM-FM} between GGA and GGA + U schemes for C-1 and C-2 doping configurations, respectively. It is found that both doping configurations are of FM ordering. Using the mean-field theory and Heisenberg model, i.e., $k_B T_C = (2/3)\Delta E_{AFM-FM}$,[23,24] we estimate the Curie temperature of the doping system. The energy difference ΔE_{AFM-FM} is large enough to lead to high temperature ferromagnetism. In Table 2, it can be seen that the interlocking N atom is polarized and has a small magnetic moment. In the ground state (FM state), the spin alignments of Mn and interlocking N atoms can be shown as Mn(↑)–N(↓)–Mn(↑) for $Zn_{22}Mn_2O_{23}N$, the intermediate spin-down N atom mediates the spin states of the two Mn atoms parallelly. In order to estimate the charge transfer between Mn and N ions, Mn-doped ZnO is also studied with GGA and GGA + U schemes, and both schemes demonstrate that Mn-doped ZnO is AFM. The magnetic moments of Mn atoms are about 4.6 μ_B and 4.8 μ_B in Mn-doped ZnO with GGA and GGA + U schemes, respectively. We consider Mn ions in the form of Mn^{2+} in Mn-doped ZnO as reported by other groups.[12,25,26] The valence electron configurations of Mn, O, and N atoms are $3d^5 4s^2$, $2s^2 2p^4$, and $2s^2 2p^3$, respectively. Therefore, the charge transfer can be estimated by comparing the magnetic moments of Mn atoms in Table 2 with those calculated by using corresponding schemes (GGA and GGA + U) in Mn-doped ZnO, respectively (e.g., for the FM state of C-1 configuration with GGA scheme, N substituting for O makes the magnetic moment of Mn to decrease from 4.6 μ_B to 4.11 μ_B, which suggests that there is about 0.5 electron from Mn 3d-shell which transfers to N^{2-} ion). In the FM state, the GGA calculations show that about 0.5 electron per Mn^{2+} ion (the remaining 0.5 electron belongs to Mn 3d-shell) transfers to the N^{2-} ion (N 2p-shell) when the N atom substitutes for the intermediate O atom of the paired Mn atoms, which leads to the high-state Mn ion (close to +2.5) and trivalent N^{3-} ion. However, in the AFM state, the GGA calculations show that

there is one electron that transfers from the downspin Mn^{2+} ion (Mn 3d-shell) to the N^{2-} ion (N 2p-shell) but no electron transfers for the upspin Mn^{2+} ion (so it remains its former valence), which causes the AFM state to possess a net magnetic moment of about 1 μ_B rather than 0 μ_B. Figure 3 shows the schematic diagram of the electron transfer between Mn and N ions in the FM and AFM states, respectively. In the FM state, the electron transfer results in the stronger exchange interaction between two Mn ions than in the AFM state: the exchange interaction lowers the kinetic energy of the system, which results in the fact that the FM state is favorable in energy. When the Coulomb interaction parameter U is added to the system, the minority- and majority-spin states of Mn 3d are pushed upward and downward, respectively, which makes the magnetic moments of Mn atoms and N atom obtained from the GGA + U scheme increased compared with from the GGA scheme (see Table 2), and the electron transfer similar to that from the GGA scheme.

Table 2. Calculated total magnetic moments of (Mn, N)-codoped ZnO supercell (M_{tot}), magnetic moments of Mn ion (M_{Mn}), N ion (M_N) and Mn-3d orbital (M_{Mn-3d}), and the energy difference ΔE_{AFM-FM} between the AFM and FM states, obtained by GGA and GGA + U schemes, respectively. The negative magnetic moments in the brackets are owned by the spin-down atoms. ($U_{Zn} = 2$ eV and $U_{Mn} = 3$ eV).

Configuration	Magnetic couple	M_{tot}/μ_B	M_{Mn}/μ_B	M_{Mn-3d}/μ_B	M_N/μ_B	ΔE_{AFM-FM}/meV
C-1	FM	8.84	4.11	4.0	–0.15	216.4
	AFM	0.97	4.47 (–3.57)	4.34 (–3.52)	0.08	
C-1 + U	FM	8.97	4.50	4.38	–0.36	260.1
	AFM	1	4.76 (–4.15)	4.63 (–4.07)	0.3	
C-2	FM	8.81	4.14	4.03	–0.15	205.3
	AFM	0.89	4.45 (–3.60)	4.32 (–3.54)	0.08	
C-2 + U	FM	8.98	4.52	4.40	–0.37	251.6
	AFM	1	4.77 (–4.15)	4.63 (–4.07)	0.3	

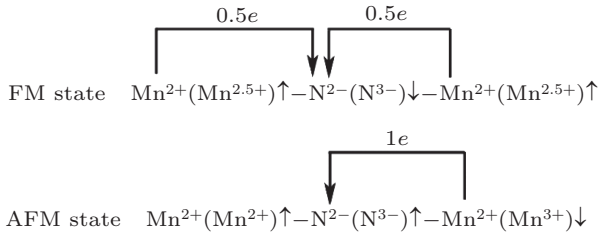


Fig. 3. (color online) Schematic diagrams of the electron transfer between Mn and N ions in the FM and AFM states respectively. The valences of Mn and N ions in the bracket are the final valences after charge transfer. The arrows indicate the spin alignments of Mn and N ions (arrows indicate up and down directions, respectively).

To further reveal the origin of FM in (Mn, N)-codoped ZnO system, we investigate the electronic structure of C-1 configuration. Figure 4(a) shows the total density of states (DOS) of the system, obtained with the GGA scheme. It can be seen that the Fermi energy passes through the spin-up density states, and there are no contributions to the DOS from the spin-down band. Therefore, the system shows the ferromagnetism and a half-metal characteristic. Figure 4(b) shows the partial DOSs of Mn 3d and N 2p states obtained with the GGA scheme. It can be seen that the Mn 3d and N 2p states overlap well. The hybridization between Mn 3d and N 2p electrons mediates the stable FM ordering. Figures 4(c) and 4(d) show the band structures of C-1 configuration obtained with the GGA + U method, at $U_{Zn} = 2$ eV and $U_{Mn} = 3$ eV. It can be seen that parameter U makes the band gap between the occupied and unoccupied Mn 3d states broader. However, the hybridization between Mn 3d and N 2p states remains almost the same as results obtained with GGA scheme (as shown in Fig. 4(d)) and the FM state is still lower in energy than the AFM state. Figure 5 shows the spin distribution for the C-1 configuration, in which the spin components are mainly distributed around the Mn–N–Mn complex. The intermediate N ion is polarized and has an opposite spin alignment to the adjacent Mn ions. The ferromagnetism is mediated through the p–d exchange interaction between carriers and Mn ions, which induces an indirect exchange interaction between Mn ions. The big values of $U_{Zn} = 3$ eV ~ 7 eV and $U_{Mn} = 4$, 5 eV are also adopted in C-1 configuration to study the effect of Hubbard U on the ground magnetic ordering in (Mn, N)-codoped ZnO system. The assumed values of the "U" contain the typical values of transition metals.[27,28] It is found that the hybridization between Mn 3d and N 2p states remains almost the same as $U_{Zn} = 2$ eV and $U_{Mn} = 3$ eV and the FM state is still lower in energy than the AFM state. Therefore, the value of "U" has little effect on the ground magnetic ordering in (Mn, N)-codoped ZnO system.

To investigate the long-range magnetic ordering, we calculate the electronic structure of (Mn, N)-codoped ZnO with two Mn and one N atoms in a $4\times4\times4$ supercell with 72 atoms. This amounts to an Mn concentration of 5.6% and the N concentration of 2.8%, and they are consistent with the experimental concentrations. In the doping supercell, the two Mn atoms and one N atom are far from each other. Results show that the FM ordering is 43.5 meV lower in total energy than the AFM ordering, indicating that the FM ordering is more stable than the AFM ordering. Therefore, (Mn, N)-codoped ZnO system can realize the long-range ferromagnetism. Later,

the magnetic property is also studied when increasing the N dopant concentration. Table 3 shows the calculated results of Mn and N at different ratios. It is found that the energy difference $\Delta E_{\mathrm{AFM-FM}}$ is somewhat reduced but still remains substantial at high N doping concentration. However, it is found that the total magnetic moment decreases with the N concentration increasing. Hence, too high N dopant concentration is not beneficial to the (Mn, N)-codoped ZnO system.

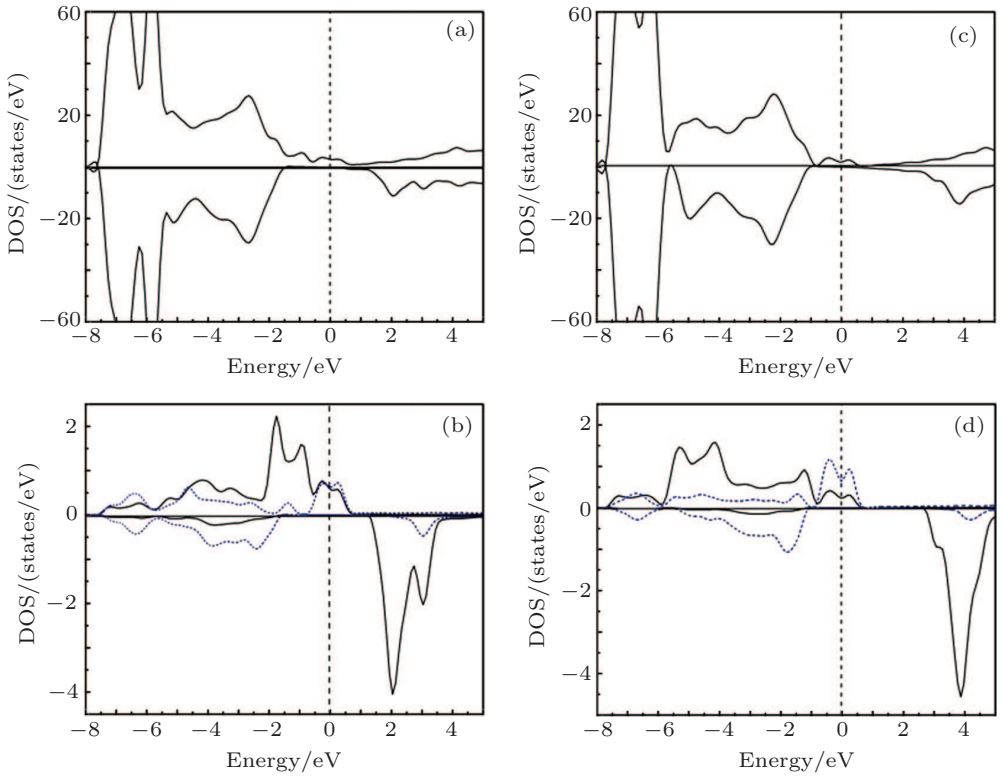


Fig. 4. (color online) The total DOSs, partial DOSs of Mn 3d and N 2p by different calculation schemes for C-1: (a) total DOSs in GGA; (b) partial spin DOSs of Mn 3d (black line) and N 2p (blue dashed line) in GGA; (c) total DOSs in GGA + U; (d) partial spin DOSs of Mn 3d (black line) and N 2p (blue dashed line) in GGA + U. The vertical dotted line denotes the Fermi level.

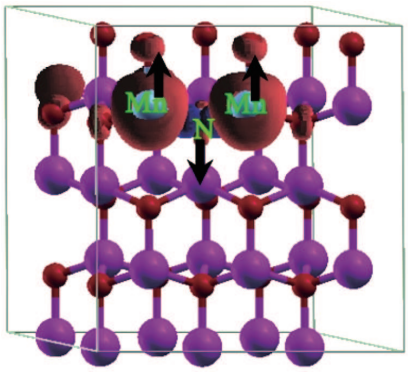


Fig. 5. (color online) Spatial spin density distribution of (Mn, N)-codoped ZnO system of C-1 in the FM ordering. The direction of arrow indicates the spin-up region and spin-down region. ($\rho = 0.008$ e/au^3).

Table 3. Calculated results of Mn and N at different ratios. The second column refers to the energy difference between AFM state and FM state, the third column the ground state of each doping configuration, and the last column the total magnetic moment.

Mn:N ratio	$E_{\mathrm{AFM-FM}}$/meV	Ground state	$M_{\mathrm{tot}}/\mu_{\mathrm{B}}$
2:1	216.4	FM	8.84
2:2	170.0	FM	7.93
2:3	79.6	FM	6.99
2:4	127.0	FM	6.00
2:5	168.6	FM	4.94

4. Conclusions

In this paper, (Mn, N)-codoped ZnO is studied by GGA and GGA + U schemes of density functional theory, and both schemes indicate that N dopant can make the system have stable ferromagnetism. The ferromagnetism is mediated through the *p–d* exchange interaction between carriers and Mn ions, which induces an indirect exchange interaction between Mn ions. However, the indirect exchange interaction of Mn–N–Mn complex is different from the Mn–O–Mn complex because the electron transfer leads to the Mn 3d-shells not half-occupied any more. Our studies demonstrate that the ferromagnetism can be explained by the p–d exchange interaction mechanism in (Mn, N)-codoped ZnO.

References

[1] Dietl T, Ohno H, Matsukura F, Cibert J and Ferrand D 2000 *Science* **287** 1019
[2] Kittilstved K R, Norberg N S and Gamelin D R 2005 *Phys. Rev. Lett.* **94** 147209
[3] Xu H Y, Liu Y C, Xu C S, Liu Y X, Shao C L and Mu R 2006 *Appl. Phys. Lett.* **88** 242502
[4] Yan W S, Sun Z H, Liu Q H, Li Z R, Shi T S, Wang F, Qi Z M, Zhang G B and Wei S Q 2007 *Appl. Phys. Lett.* **90** 242509

[5] Gu Z B, Lu M H, Wang J, Wu D, Zhang S T, Meng X K, Zhu Y Y, Zhu S N and Chen Y F 2006 *Appl. Phys. Lett.* **88** 082111

[6] Ruan H B, Fang L, Li W J, Qin G P, Wu F and Kong C Y 2014 *Mater. Sci. Semicond. Process.* **21** 52

[7] Wu K P, Gu S L, Tang K, Ye J D, Zhu S M, Zhou M R, Huang Y R, Xu M X, Zhang R and Zheng Y D 2012 *J. Magn. Magn. Mater.* **324** 1649

[8] Wang D D, Xing G Z, Yan F, Yan Y S and Li S 2014 *Appl. Phys. Lett.* **104** 022412

[9] Wu K P, Gu S L, Zhu S M, Huang Y R and Zhou M R 2012 *Acta Phys. Sin.* **61** 057503 (in Chinese)

[10] Yang T Y, Kong C Y, Ruan H B, Qin G P, Li W J, Liang W W, Meng X D, Zhao Y H, Fang L and Cui Y T 2012 *Acta Phys. Sin.* **61** 168101 (in Chinese)

[11] Assadi M H N, Zhang Y B and Li S 2009 *J. Phys.: Condens. Matter* **21** 185503

[12] Wang Q, Sun Q and Jena P 2004 *Phys. Rev. B* **70** 052408

[13] Zhao L, Lu P F, Yu Z Y, Guo X T, Shen Y, Ye H, Yuan G F and Zhang L 2010 *J. Appl. Phys.* **108** 113924

[14] Giannozzi P, Baroni S, Bonini N, Calandra M, Car R, Cavazzoni C, Ceresoli D, Chiarotti G L, Cococcioni M, Dabo I, Dal Corso A, Fabris S, Fratesi G, de Gironcoli S, Gebauer R, Gerstmann U, Gougoussis C, Kokalj A, Lazzeri M, Martin-Samos L, Marzari N, Mauri F, Mazzarello R, Paolini S, Pasquarello A, Paulatto L, Sbraccia C, Scandolo S, Sclauzero G, Seitsonen A P, Smogunov A, Umari P and Wentzcovitch R M 2009 *J. Phys.: Condens. Matter* **21** 395502

[15] Perdew J P, Burke K and Ernzerhof M 1996 *Phys. Rev. Lett.* **77** 3865

[16] Monkhorst H J and Pack J D 1976 *Phys. Rev. B* **13** 5188

[17] Pack J D and Monkhorst H J 1977 *Phys. Rev. B* **16** 1748

[18] Methfessel M and Paxton A T 1989 *Phys. Rev. B* **40** 3616

[19] Hu S J, Yan S S, Zhao M W and Mei L M 2006 *Phys. Rev. B* **73** 245205

[20] Shen L, Wu R Q, Pan H, Peng G W, Yang M, Sha Z D and Feng Y P 2008 *Phys. Rev. B* **78** 073306

[21] Ye X J, Song H A, Zhong W, Xu M H, Qi X S, Jing C Q, Yang Z X, Au C T and Du Y W 2008 *J. Phys. D: Appl. Phys.* **41** 155005

[22] Peng X Y and Ahuja R 2009 *Appl. Phys. Lett.* **94** 102504

[23] Yang K S, Wu R Q, Shen L, Feng Y P, Dai Y and Huang B B 2010 *Phys. Rev. B* **81** 125211

[24] Kudrnovský J, Turek I, Drchal V, Máca F, Weinberger P and Bruno P 2004 *Phys. Rev. B* **69** 115208

[25] Mahmoud A B, von Bardeleben H J, Cantin J L, Mauger A, Chikoidze E and Dumont Y 2006 *Phys. Rev. B* **74** 115203

[26] Droubay T C, Keavney D J, Kaspar T C, Heald S M, Wang C M, Johnson C A, Whitaker K M, Gamelin D R and Chambers S A 2009 *Phys. Rev. B* **79** 155203

[27] Gopal P and Spaldin N A 2006 *Phys. Rev. B* **74** 094418

[28] Cococcocioni M and de Gironcoli S 2005 *Phys. Rev. B* **71** 035105